$Zr_{0.05}Ti_{0.95}O_2$-Functionalized Porous SiO_2/Glass Fiber Composite Filter-Papers for Efficient $PM_{2.5}$ Capture and Photocatalytic Toluene Degradation

*Wenqing Feng, Jingyue Bi, Haoyu Zhang, Ning Wang, Lin Fan, Yichao Ling, Haojie Lan, Xu Qiao, Zhaoyang Fei**

[a] State Key Laboratory of Materials-Oriented Chemical Engineering, College of Chemical Engineering, Nanjing Tech University, Nanjing 211816, PR China

---

Corresponding Authors

** E-mail: zhaoyangfei@njtech.edu.cn (Z. Fei).*

1. Experimental

1.1 Preparation of SiO_2 Microspheres. SiO_2 microspheres were synthesized via a two-step acid-base catalyzed sol-gel method using methyltrimethoxysilane (MTMS) as the silicon precursor. In a typical procedure, 14.6 mL of MTMS was mixed with 100 mL of methanol in a beaker. Separately, 0.01 g of oxalic acid, serving as an acidic catalyst, was dissolved in 50 mL of distilled water. This aqueous solution was then poured into the beaker containing the MTMS/methanol mixture. The resulting mixture was stirred at room temperature for 2 h, followed by the addition of 3.8 mL of N,N-dimethylformamide (DMF). Subsequently, 9 mL of ammonia aqueous solution was added, and stirring was continued for 10 min. The solution was then transferred to an oil bath and subjected to gelation at 40 °C for 30 min. After complete gelation, the temperature of the oil bath was raised to 50 °C, and the gel was aged for 24 h. The resulting product was washed with n-hexane 3-4 times and finally dried in an oven at 80 °C for 24 h to obtain S-9 SiO_2 microspheres. A series of S-n SiO_2 microspheres with different ammonia water addition amounts (5, 7, 9, 11 mL) were prepared using the same method, where 'n' denotes the volume of ammonia used. The ammonia dosage was varied to tune the particle size and morphology of the SiO_2 microspheres by regulating the base-catalyzed condensation process.

1.2 Preparation of the Binder. MTMS was added to a 500 mL beaker and stirred using a magnetic stirrer. A diluted phosphoric acid solution, prepared by mixing 72 mL of distilled water with 0.5 mL of phosphoric acid, was then added dropwise to the beaker. The mixture was stirred at room temperature for 1 h to hydrolyze the MTMS. The resulting solution was transferred to a flask and heated in an oil bath at 60 °C for 30 min. It was then returned to a beaker and cooled at room temperature for 1 h, yielding a highly viscous solution which served as the binder.

1.3 Preparation of $Zr_xTi_{1-x}O_2$ Catalytic Materials. $Zr_xTi_{1-x}O_2$ was prepared by a mixed sol-gel and freeze-drying method. Typically, 2.5 mL of tetrabutyl titanate was added to 6.5 mL of ethanol in Beaker A and stirred vigorously. Meanwhile, a solution was prepared in Beaker B by mixing 0.8 mL of distilled water, 2 mL of ethanol, and 1.2 mL of acetic acid. Solution B was then added dropwise to Solution A under continuous stirring. After 5 min of additional stirring, 0.25 mL of formamide was introduced into the mixture. The resulting mixture was aged in an oil bath at 70 °C for 6 h to obtain a TiO_2 gel. This gel was then transferred into a 50 mL Teflon-lined autoclave, immersed in acetone, and hydrothermally treated at 120 °C for 21 h. After cooling, the product was washed with ethanol to remove residual acetone. The purified gel was pre-frozen for 2 h and then freeze-dried under vacuum for 2 days, yielding a TiO_2 aerogel designated as TiO_2. Next, 1 g of the TiO_2 aerogel was immersed in a 5.0 wt.% $ZrO(NO_3)_2$ solution at room temperature for 1 h with stirring. The solid was collected and dried in an oven at 100 °C. Finally, the resulting powder was calcined in a muffle furnace at 300 °C for 1 h. The obtained catalyst was named $Zr_{0.05}Ti_{0.95}O_2$. Using the same procedure, a series of $Zr_xTi_{1-x}O_2$ catalysts with different Zr mass concentrations (0.5, 1.0, 5.0 wt.%) were synthesized, where 'x' represents the nominal Zr mass fraction.

2. Characterization

2.1 Characterization Methods of Catalysts

X-ray diffraction (XRD) was used to characterize the phase components on the Smart Lab diffractometer of Rigaku, Japan. The ray source was Cu Kα (λ=0.154 nm), the tube current and voltage of 40 mA and 40 kV, the scanning range is 5-80°, and the step size is 0.02°. The scanning speed is 20° min^{-1}.

Scanning electron microscope (SEM) was used to characterize the S-8200 instrument of Japan Hitachi Co., LTD., with an operating voltage of 20 kV, to observe the microstructure of the surface of the material. The samples were all treated with gold spraying before the experiment.

N_2 adsorption-desorption was characterized by 3Flex adsorption from Micromeritics. Before testing and analysis, 100 mg samples were pre-treated with vacuum degassing at 60°C for 4 h before testing.

The specific surface area of the sample was calculated by BET equation, and the pore diameter (D_p) and pore volumewere (V_p) calculated by BJH model.

Thermogravimetric analysis (TGA) was performed on a TGA/DSC 3+ thermal analyzer

(Mettler Toledo, Switzerland). The temperature was increased from 25 to 800 °C at a heating rate of 10 °C min^{-1} under an air atmosphere.

The air permeability and average pore diameter of the filter-paper were measured in N_2 atmosphere by the aperture tester ipore-1500 of PMI. The transmitted infrared was tested on the American Thermo company's Nicolet IS50 FTIR spectrometer. During the test, potassium bromide was pressed into thin slices, the spectral background was collected at room temperature, and then the sample atlas was collected. The scanning range was 400-4000 cm^{-1}, and the scanning times were 32.

Tensile tests were performed using an XLW(EC)-A electronic universal testing machine (China Blu-ray Electromechanical Technology Co., Ltd.). The tests were conducted at 25 °C and 40% relative humidity. Rectangular specimens (18.0 mm × 15.0 mm × 0.15 mm) were used. The crosshead speed was set to 2 mm min^{-1} and the load cell capacity was 10 N. The gauge length was defined as the exposed length between the grips. Each sample was measured three times to minimize experimental error.

Static water contact angles were measured using a Dropmeter A-100 contact-angle goniometer (Haishu Meisu, China) to evaluate the wettability of the samples.

The contact Angle was the Angle between the tangent line of the interface between the gas-liquid phase and the boundary between the solid-liquid phase at the intersection of the solid-liquid phase.

The ICP of the samples was determined using the OPTIMA7000DV equipment from Perkin Elmer Company in the United States. The sample powders were dissolved in dilute HNO_3 solution, and the content was measured according to the standard curves of each element.

The UV-Vis DRS spectra of all samples were measured using a Perkin Elmer Lambda 365 UV-Vis spectrophotometer. $BaSO_4$ was used as the reference material, and the catalyst samples were pressed onto the surface of $BaSO_4$ for measurement over the range of 300-800 nm.

UV-vis diffuse reflectance spectroscopy (UV-vis DRS) spectra of all samples were recorded using a Lambda 365 UV-vis spectrophotometer (PerkinElmer, USA). $BaSO_4$ was used as the reflectance reference, and the catalyst powders were gently pressed onto the surface of $BaSO_4$ for measurement. The spectra were collected over a wavelength range of 300-800 nm.

Furthermore, the optical band gap energy (Eg) of the catalysts was estimated from the UV-vis absorption spectra based on the relationship between the absorption coefficient (α) and the incident photon energy (hν), as expressed by the following equation:

$$\alpha h\upsilon = B_d(h\upsilon - E_g)^n \tag{S1}$$

where α is the absorption coefficient, hν is the photon energy, Bd is a constant, and n depends on the nature of the electronic transition (n = 2 for indirect allowed transitions and n = 1/2 for direct allowed transitions). The band gap energy was determined by extrapolating the linear region of the plot of $(\alpha h\nu)^2$ versus hν to the energy axis.

2.2 Physical Performance Indicators of Filter-Paper Materials

Detachment Resistance Measurement. A flexible filter-paper sample with an initial mass of W_1 was placed in a beaker containing deionized water and subjected to ultrasonic treatment for 20 min. Subsequently, the sample was removed, dried in an oven, and weighed again, with the final mass recorded as W_2. The detachment rate was calculated according to Equation (S2):

$$N\ (\%) = \frac{W_1 - W_2}{W_1} \times 100\% \tag{S2}$$

Acid-Alkali Corrosion Measurement. A flexible filter-paper sample with an initial mass of G_1 was immersed separately in 5% sodium hydroxide (NaOH) and 5% sulfuric acid (H_2SO_4) solutions for 24 h. After immersion, the sample was rinsed thoroughly with deionized water, dried in an oven, and then weighed. The final mass was recorded as G_2. The corrosion rate was calculated according to Equation (S3):

$$S\ (\%) = \frac{G_1 - G_2}{G_1} \times 100\% \tag{S3}$$

2.3 $PM_{2.5}$ filtration test

The $PM_{2.5}$ filtration performance of all filter-papers was evaluated using a homemade closed testing setup. The device consists of two chambers separated by a circular opening (2.5 cm in diameter), where the flexible porous filter-paper was mounted. Cigarette smoke was introduced from a connected combustion chamber as the $PM_{2.5}$ source and continuously passed through the filter. The particle concentration in the combustion chamber was monitored using a dust particle counter. During the test, the initial $PM_{2.5}$ concentration was recorded as X_0. The airflow rate was controlled at 3 L min^{-1}, and filtration was conducted for 20 min, after which the $PM_{2.5}$ concentration was measured again and denoted as X_1. In addition, a differential pressure gauge was connected to the upstream and downstream ports to record the inlet and outlet pressures (P_{in} and P_{out}), from which the pressure drop (ΔP) was obtained. The filtration efficiency (η) and pressure drop (ΔP) were calculated according to Eqs. (S4) and (S5).

$$PM_{2.5}\, filteration\ efficiency(\eta) = (1 - \frac{X_1}{X_0}) \times 100\% \tag{S4}$$

$$\Delta P = P_{in} - P_{out} \tag{S5}$$

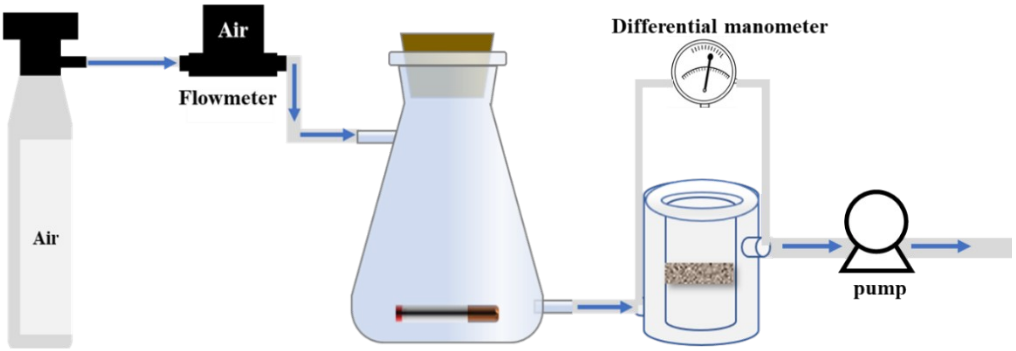

Fig.S1 Material filtration performance evaluation system.

2.4 Photocatalytic test

The photocatalytic activity of the $Zr_xTi_{1-x}O_2$/S/G fiber filter-papers for toluene degradation was assessed in a custom-built photocatalytic reaction system. The reactor features an internal diameter of 5 cm, with the upper and lower sections having heights of 15 cm and 35 cm, respectively. These sections are sealed together using a compression seal. A filter-paper sample (containing the TiO_2-based active component) was cut into a 5 cm diameter disc and mounted inside the photocatalytic reactor.

A three-stream air supply system was employed: one stream carried toluene via an air bubble, another carried water vapor via a separate air bubble, and the third was a diluting air stream. These streams were then mixed to generate the reactant gas, with the toluene concentration set at 100 ppm and a total flow rate of 101 mL min^{-1}. A 300 W xenon lamp (CEL-HXF300-T3), equipped with a filter to provide UV light (intensity: 200 mW cm^{-2}), was used as the light source and positioned above the photo-reactor. For visible-light tests, the same xenon lamp equipped with a 420 nm cutoff filter was used unless otherwise stated. For formaldehyde-removal tests, the same reactor configuration and operating conditions were used unless otherwise stated, with an inlet formaldehyde concentration of 100 ppm. The conversion of toluene was analyzed using an online gas chromatograph (NBGC-60). The toluene conversion (%), was calculated using Equation (S6).

The catalyst reusability was also tested. After one activity test, the light source was turned off, while the sample was kept in the reactor without removal, and the system was allowed to stabilize for 20 min under continuous supply of the mixed gas before the next activity test was initiated. Each photocatalytic cycle lasted for 60 min under irradiation. The xenon lamp was then switched on to initiate the next activity test. This cycle was repeated six times to evaluate the catalyst's stability.

$$The\ toluene\ conversion\ (\%) = \frac{C_{in} - C_{out}}{C_{in}} \times 100\% \qquad \text{(S6)}$$

The inlet toluene concentration was estimated as

$$C_{Toluene}\ (ppm) = \frac{P_b \times \frac{V_x}{V_0}}{P_0} \times 10^6 \qquad \text{(S7)}$$

where:

V_x-Flow rate of the entrainment gas (mL min^{-1});

V_0-Total flow rate of the mixed gas (mL min^{-1});

P_0-Standard atmospheric pressure (101.325 kPa);

P_b-Saturation vapor pressure of toluene at 0 °C (0.914 kPa).

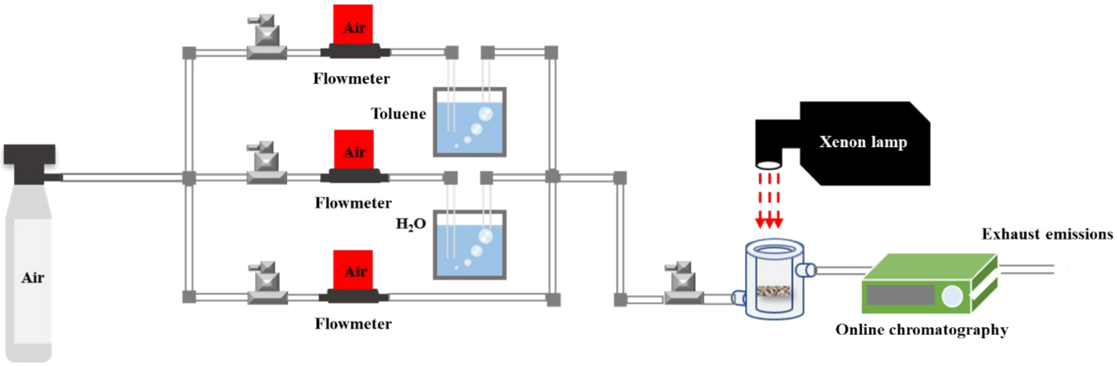

Fig.S2 Evaluation system of photocatalytic activity over materials.

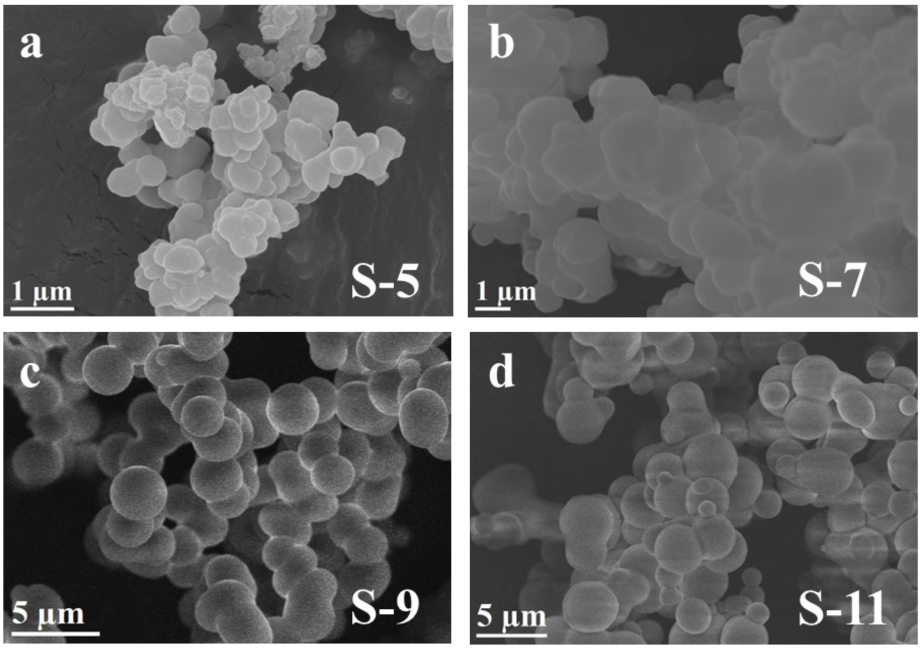

Fig. S3. SEM images of S-n microspheres.

(a: S-5; b: S-7; c: S-9; d: S-11)

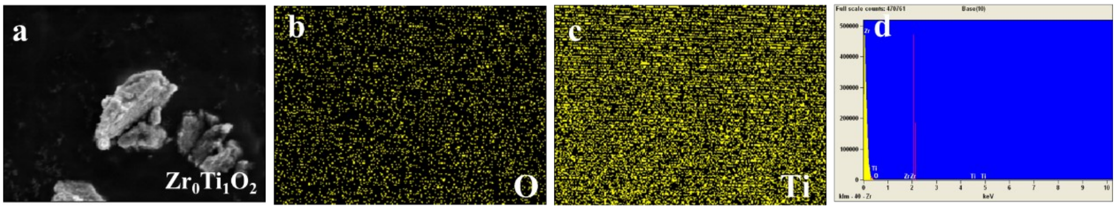

Fig. S4. SEM images and elemental mapping of $Zr_0Ti_1O_2$ catalysts.

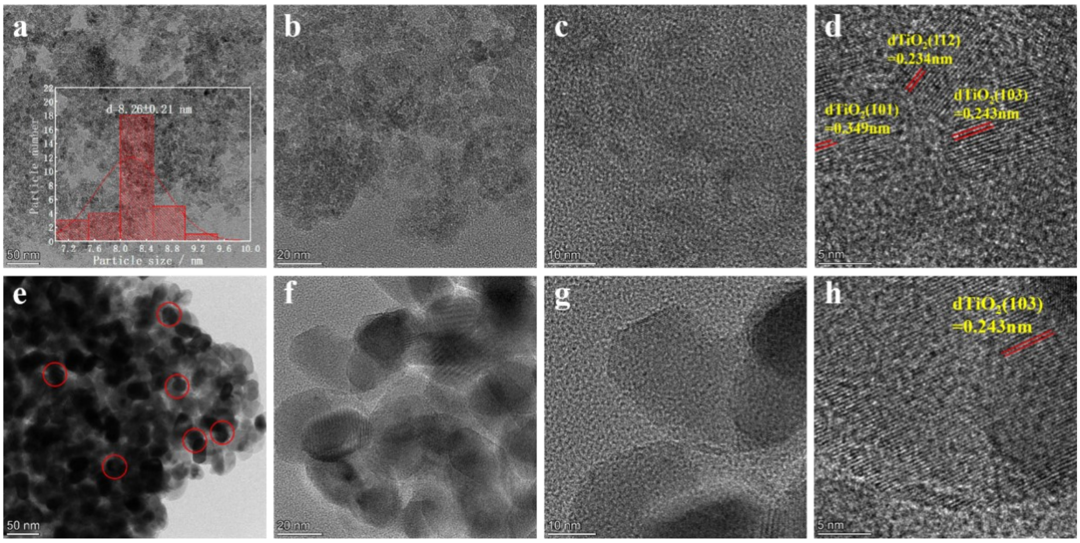

Fig. S5. TEM images of TiO_2-SY and $Zr_0Ti_1O_2$ catalysts.

(a, b, c, d: $Zr_0Ti_1O_2$; e, f, g, h: TiO_2-SY)

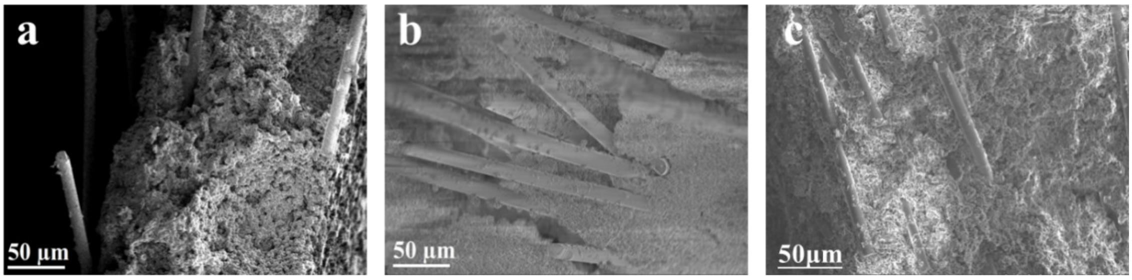

Fig. S6. SEM images of $Zr_{0.05}Ti_{0.95}O_2$/S/G filter-papers.

（a: $Zr_{0.05}Ti_{0.95}O_2$/S/G-1; b: $Zr_{0.05}Ti_{0.95}O_2$/S/G-2; c: $Zr_{0.05}Ti_{0.95}O_2$/S/G-3）

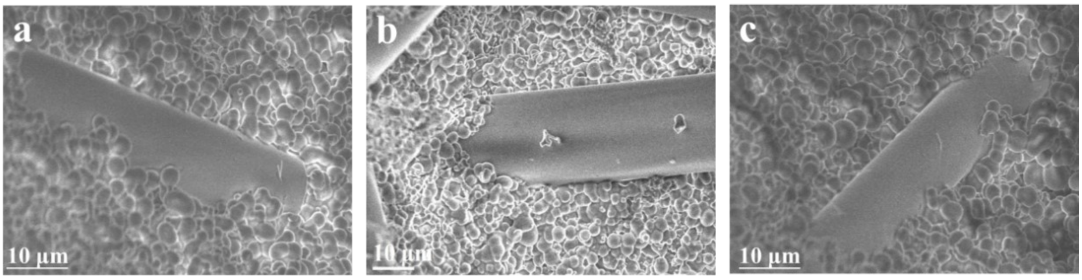

Fig. S7. SEM images after acid corrosion treatment of $Zr_{0.05}Ti_{0.95}O_2$/S/G filter-papers.

（a: $Zr_{0.05}Ti_{0.95}O_2$/S/G-1; b: $Zr_{0.05}Ti_{0.95}O_2$/S/G-2; c: $Zr_{0.05}Ti_{0.95}O_2$/S/G-3）

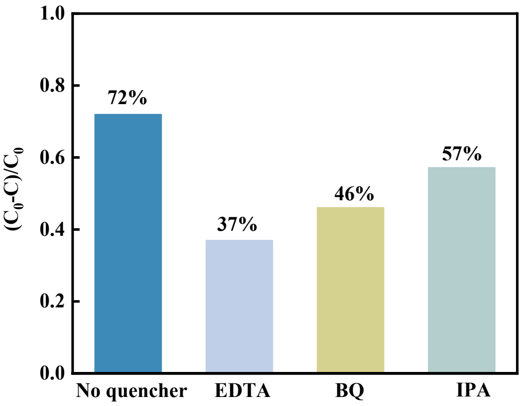

Fig. S8. The removal rate of toluene over the $Zr_{0.05}Ti_{0.95}O_2$ using different quenchers.

Table S1. Comparison of the airflow resistance of the present integrated filter-paper with representative commercial air filters.

Filter	Main function	Filter grade / efficiency	Test airflow condition	Initial pressure drop (Pa)	Source
$Zr_{0.05}Ti_{0.95}O_2$/S/G-2	$PM_{2.5}$ filtration + VOC photocatalytic removal	$PM_{2.5}$ 94.32%	0.10 m s⁻¹	140.7	This work
Representative Commercial panel filter (MERV 13)	Particulate removal	MERV 13 / ePM10 60%	3400 m³ h⁻¹	85-100	Commercial datasheet
Representative Commercial bag filter (Hi-Flo)	Particulate removal	ePM1 60-85%	3400 m³ h⁻¹	65-160	Commercial datasheet
Representative Commercial combined filter (CityPleat)	Particulate + molecular removal	Coarse 65%	1700-3400 m³ h⁻¹	90-140	Commercial datasheet
Representative commercial HEPA filter (H13)	Fine particle removal	H13	258-2912 m³ h⁻¹	250-290	Commercial datasheet

Note: The commercial-filter data are included only as representative references. Direct one-to-one comparison is limited by differences in filter configuration and testing conditions.

Table S2. Comparison of the present $Zr_{0.05}Ti_{0.95}O_2$/S/G-2 filter-paper with representative multifunctional filters for simultaneous PM and VOC removal.

Material	PM metric	Pressure drop	VOC species	VOC conversion	Test condition	Ref.
$Zr_{0.05}Ti_{0.95}O_2$/S/G-2 composite filter-paper	94.32%	140.7-148.7 Pa	Toluene	72%	0.10 m s^{-1}	This work
MIL-125-NH_2-coated electret filter media (E-MOFilter)	91.11% (0.3 μm particle)	4.5 Pa	Toluene	72%	5 cm s^{-1}	[1]
p-BWO@MIL-coated electret filter media (PE-MOFilter)	85%	negligible increase of pressure drop	Toluene	68.7%	5 cm s^{-1}	[2]
1%Ag-TiO_2-silk multifunctional air filter	99.04%	34.33 Pa	Formaldehyde	98.3%	PM test in a sealed custom box	[3]
Cu_2O/TiO_2-coated ceramic catalyst filter (CCF)	95%	20 Pa	Formaldehyde	82%	linear velocity 0.12 m s^{-1}	[4]

References:

1. Y. Zhang, X. He, Z. Zhu, W. N. Wang and S. C. Chen, Simultaneous removal of VOCs and $PM_{2.5}$ by metal-organic framework coated electret filter media, J. Membr. Sci., 2021, 618, 118629.

2. Y. Zhang, Z. Zhu, W. N. Wang and S. C. Chen, A Novel Sustainable Semiconductor/Metal-organic Framework Coated Electret Filter for Simultaneous Removal of $PM_{2.5}$ and VOCs, Aerosol Air Qual. Res., 2023, 23.

3. S. Wanwong, W. Sangkhun, P. Jiamboonsri, and T. Butburee, Electrospun silk nanofiber loaded with Ag-doped TiO_2 with high-reactive facet as multifunctional air filter, RSC Adv., 2023, 13(37), 25729-25737.

4. H. J. Kwon, D. S. Yang, M. S. Koo, S. M. Ji, J. Jeong, S. Oh, S. K. Kuk, H. Heo, D. J. Ham, M. Kim, H. Choi, J.-M. Lee and H. C. Lee, Long-lifetime water-washable ceramic catalyst filter for air purification, Nat. Commun., 2023, 14, 520.